Fluctuations in the coil-stretch transition of flexible polymers in good solvents: A peak due to nonlinear force relation

Rangarajan Radhakrishnan and Patrick T. Underhill

Phys. Rev. E **88**, 012606 — Published 24 July 2013

DOI: 10.1103/PhysRevE.88.012606

Fluctuations in the coil-stretch transition of flexible polymers in good solvents: A peak due to non-linear force relation.

Rangarajan Radhakrishnan and Patrick T. Underhill*

Department of Chemical and Biological Engineering, Rensselaer Polytechnic Institute, 110 8th St, Troy, New York 12180, USA

Abstract

Long flexible polymers undergo a coil to stretch transition (CST) in an elongational flow. Near the CST, a peak can be observed in the fluctuations of the size of a molecule ($|R|$). Solvent effects on the fluctuations are studied using Brownian Dynamics simulations of a non-linear spring force relation that can represent real molecules. Ignoring the influence of hydrodynamic interactions, a linear region in the spring force relation is known to cause the peak in $|R|$ fluctuations. In contrast, we find that a peak in the fluctuations can be obtained even for the non-linear spring force relation. We analyze the influence of hydrodynamic interactions on the fluctuations using a dumbbell model with a conformation dependent drag coefficient.

* Corresponding author: underhill@rpi.edu

I. INTRODUCTION

Flow behavior of dilute polymer solutions are of fundamental interest for many applications. Recently, there has been considerable interest in stretching polymers for analysis using microfludic devices[1–3]. Dilute polymer solutions in elongational flow have also been analyzed to understand turbulent drag reduction[4, 5]. In elongational flows, polymers in dilute solutions undergo a coil-stretch transition (CST) at a critical strain rate[6, 7]. The existence of the CST and hysteresis in the transition have been confirmed by direct and indirect measurements in dilute polymer solutions [8, 9]. Since it is difficult to determine a critical strain rate $\dot{\epsilon}_c$ from a plot of extension vs. strain rate for some molecules, a peak in extension fluctuations has been used to quantify $\dot{\epsilon}_c$ [10]. Recently, Tang et al. [1] have found that changes in the force-extension behavior of a molecule due to confinement in a channel lead to changes in the CST. Two different linear regions in the force-extension relation of the polymer gave rise to two different critical strain rates, which were identified by the peaks in the fluctuations.

The force extension (FE) behavior of a molecule is affected by solvent-polymer interactions [11–14]. The role of repulsive solvent polymer interactions on the FE of a polymer is determined by the excluded volume parameter v/l^3 and the number of Kuhn steps N_K. Effective repulsive interactions between the polymer segments (mediated by the solvent) can give rise to a non-linear scaling relation $f \sim R^{3/2}$ between force f and extension R for long molecules with $N_K \gtrsim \mathcal{O}(10^4)$. The effect is most pronounced when $v/l^3 \sim \mathcal{O}(1)$. This change in the FE of a molecule leads to changes in the CST [15, 16].

In this article, we analyze the effect of the non-linearity in FE on the fluctuations, to better understand the ability of fluctuations to identify the changes in the CST. We show that a peak in the fluctuations can be obtained even for a non-linear spring force relation, which does not have a sharp CST, using bead-spring chain models ignoring hydrodynamic interactions (HI). We find that the peak in the fluctuations is enhanced due to conformation dependent drag by including HI using a dumbbell model.

II. MODEL

In a bead-spring chain model, the bead positions are tracked and they are the points where the hydrodynamic forces are applied. Springs between the beads represent the change of free energy of the chain as regions of the polymer are stretched. In the Brownian dynamics (BD) methodology the beads obey a stochastic differential equation which averages over the faster motions of the solvent [17]. The solvent contributes through a viscous drag contribution, Brownian forces, and effects on the elasticity of the polymer. The stochastic equation for the change in the position of bead i is

$$d\boldsymbol{r}_i = \left(\boldsymbol{u}(\boldsymbol{r}_i) + \frac{1}{k_B T} \sum_{j=1}^{N_b} \boldsymbol{D}_{ij} \cdot \boldsymbol{F}_j + \sum_{j=1}^{N_b} \frac{\partial}{\partial \boldsymbol{r}_j} \cdot \boldsymbol{D}_{ij} \right) dt + \sqrt{2} \sum_{j=1}^{N_b} \boldsymbol{B}_{ij} \cdot d\boldsymbol{W}_j \tag{1}$$

where N_b is the number of beads, $\boldsymbol{r}_i$ is the position of bead i, $\boldsymbol{u}$ is the external fluid flow evaluated at the position of the bead, $\boldsymbol{D}_{ij}$ is the ij block of the hydrodynamic diffusion tensor, $\boldsymbol{F}_j$ is the net of spring forces and excluded volume forces on bead j, k_B is Boltzmann's constant, T is the absolute temeprature, and each $d\boldsymbol{W}_j$ is a vector of independent random variables with zero mean and variance dt where dt is the timestep. In order to satisfy the fluctuation-dissipation theorem, the tensor $\boldsymbol{B}_{ij}$ must obey

$$\boldsymbol{D}_{ij} = \sum_{k=1}^{N_b} \boldsymbol{B}_{ik} \cdot \boldsymbol{B}_{jk}^T \tag{2}$$

In this work, we will not be considering direct hydrodynamic interactions between the beads, which makes the tensors $\boldsymbol{D}_{ij}$ and $\boldsymbol{B}_{ij}$ diagonal and are given by

$$\boldsymbol{D}_{ij} = \delta_{ij} \frac{k_B T}{\zeta_i} \boldsymbol{I} \tag{3}$$

$$\boldsymbol{B}_{ij} = \delta_{ij} \left(\frac{k_B T}{\zeta_i} \right)^{1/2} \boldsymbol{I} \tag{4}$$

where δ_{ij} is the Kroneker delta, ζ_i is the drag coefficient of bead i, and $\boldsymbol{I}$ is the 3×3 identity tensor. In the first part of the article, we examine bead-spring chain models in which the bead drag coefficients are constants. Because ζ_i for each bead is constant, the divergence of the diffusion tensor is zero. In the second part we examine a dumbbell model in which the drag coefficient of each bead depends on the extension of the spring. Since we use a simple linear dependence of ζ_i on the spring extension Q, we can take the divergence of the diffusion tensor analytically. We use this model to examine the response of a polymer in

uniaxial extensional flow. This external flow $\boldsymbol{u}$ appears in the dynamical equation for each bead. The strength of the flow is measured by an extensional rate $\dot{\epsilon}$ which determines the velocity components as $u_x = -\dot{\epsilon}x/2$, $u_y = -\dot{\epsilon}y/2$, $u_z = \dot{\epsilon}z$, where here x, y, and z denote the components of the velocity and position vectors in space.

The goal in this article is to understand how the non-linear force relation for flexible polymers in good solvents affects the polymer fluctuations. A coarse-grained model has been developed previously [15, 16] that can capture the effects of solvent-polymer interactions on the elongational flow behavior of polymers. We briefly review that model here when a single spring is used. The detailed procedure for larger numbers of springs is described in ref. [15]. This model differs from a conventional model by incorporating all or most of the solvent quality effects into the spring force relation instead of as direct excluded volume repulsions between the beads. One key advantage of this model is that it can capture the elasticity of a polymer chain with very few beads, which makes it easier to analyze theoretically and compute the response in a computationally efficient way. The model incorporates the intra-spring excluded volume (ISEV) interactions into a spring force relation which is given by

$$F_{\mathrm{ISEV}}(Q) = \frac{AQ^{3/2}}{1 + BQ^{1/2}} \frac{1}{1 - (Q/Q_0)^2} \ , \tag{5}$$

where Q is the distance separating the beads of a spring, $Q_0 = N_K l$ is the contour length of the spring, and l is the Kuhn length. This functional form is an approximation that is able to capture the response of a wide range of molecules depending on the parameters A and B. We previously used a blob theory to determine A and B [15]. For extensions of the spring $B^{-1/2} \ll Q \ll Q_0$ the force is proportional to the spring length with spring constant A/B. At these extensions the force is not affected by solvent quality or finite extensibility but is determined by the θ condition parameters. With this ratio constrained, A and B are determined once one of them is set. For molecules in very good solvents, blob theory can determine A up to a order one prefactor. In order to determine that prefactor, we have used the equilibrium size of the polymer coil at equilibrium. Using these conditions gives

$$A = \frac{(2.409/\sqrt{z} + 2.122/z)\, k_B T}{R_\theta^{5/2}} \ , \tag{6}$$

$$B = \frac{2.409/\sqrt{z} + 2.122/z}{3R_\theta^{1/2}} \ , \tag{7}$$

where $R_\theta = N_k^{1/2} l$ is the θ solvent equilibrium size and the z here is the solvent quality parameter that is given by

$$z = \left(\frac{3}{2\pi}\right)^{3/2} \frac{v}{l^3}\sqrt{N_k} \ . \tag{8}$$

This model represents the FE of many polymers ranging from good to theta solvents using a dumbbell. Note that this model does not explicitly contain a linear region in FE at low force, but has the dependence of $F_{ISEV} \sim Q^{3/2}$. However, its FE behavior compares favorably with previous Monte-Carlo simulations of molecules in good solvents [15]. Therefore, we use this simple model to analyze the role of solvent interactions on fluctuations. For a bead-spring chain model of $F_{\rm ISEV}$ springs, the spring contains the intra-spring excluded volume (ISEV) contribution and the excluded volume between the springs is given by a repulsive potential modeled by a Gaussian. In comparison to $F_{\rm ISEV}$ springs, we use a model of a polymer consisting of FENE springs [18] with Gaussian potentials to model the excluded volume (EV). The FENE spring force is given by

$$F_{\rm FENE} = \frac{3k_BT}{R_\theta^2}\frac{Q}{1-(Q/Q_0)^2} \ . \tag{9}$$

Since the force-extension behavior of molecules at large forces does not depend on solvent interactions and could be molecule specific, we model the high force extension to match the behavior of a freely jointed chain by use of a FENE part in the spring force.

The focus here is on the fluctuations of the molecule in elongational flow. The fluctuations are defined as

$$\sigma = \sqrt{\langle(|R| - \langle|R|\rangle)^2\rangle} \ , \tag{10}$$

where $|R|$ is the magnitude of the end to end distance of the bead-spring chain or the dumbbell. A peak in σ corresponds to a peak in the experimental measurements of maximum projected length fluctuations [1].

III. RESULTS AND DISCUSSION

To understand the role of spring force relation or the force extension behavior of a molecule in determining σ, we first examine the case in which the hydrodynamic interactions between segments of the chain are not included. Consider a molecule such as ds-DNA molecule with $v/l^3 = 0.01$ and $N_K = 10^4$. This molecule has a peak in σ as shown

in Fig. 1 (a). The strain rate $\dot{\epsilon}$ is scaled by the theta solvent polymer relaxation time $\lambda_\theta = \zeta_0 N_K l^2/(24 k_B T \sin^2[\pi/(2N_b)])$, where ζ_0 is the drag coefficient of a bead and N_b is the number of beads in the chain, to give a Weissenberg number $\mathrm{Wi} = \dot{\epsilon}\lambda_\theta$. It is known that a polymer in θ conditions undergoes a CST near a critical Wi=0.5 [19]. The peak in σ for the ds-DNA molecule occurs near this critical Wi. Since the molecule is near θ conditions, the fluctuations calculated from BD simulations of the two models F_{FENE} and F_{ISEV} are almost identical. A multi-bead spring chain model also shows the same peak in the fluctuations. Increasing the discretization of the model from 1 to 20 springs slightly alters the high Wi fluctuations. This slight change at high Wi is because the drag on the chain from the flow only occurs at the beads, and is essentially the same phenomenon described previously [20]. The tension on the polymer is nonuniform due to the flow, but a dumbbell model only has one value of the tension, since it only has one spring. This leads to a change in response of the model if the number of beads is smaller than about 10 to 20.

The fluctuations are very different for a molecule like ss-DNA with $v/l^3 = 1$ and $N_K = 10^4$, for which F_{ISEV} does not have a significant linear region. Instead, the spring force has a wide region in which the force scales as $f \sim Q^{3/2}$. BD simulations of F_{ISEV} springs shown in Fig. 1 (b) have a peak in σ, but at a $\mathrm{Wi} < 0.5$. Increasing the discretization of this model from 1 to 20 springs does not change the value of the peak. The results of F_{FENE} springs with excluded volume potentials between the beads are very different. The fluctuations show a peak at a $\mathrm{Wi} = 0.5$. With increasing number of springs the value of this peak decreases and σ at low Wi increases. This response is because the force-extension of a F_{FENE} chain with EV has a large linear region, with the width of the linear region decreasing with increasing numbers of springs [15]. It is possible that a large number of F_{FENE} springs with EV will have the same response as that of the F_{ISEV} springs, but the number of springs needed or accuracy of an extrapolation are unknown.

We can better understand the fluctuations by using analytical expressions valid for low and high Wi, which were shown in Fig. 1. For a dumbbell model, not including conformation dependent drag, the probability distribution of the dumbbell in flow follows a Boltzmann distribution in which there is an extra contribution to the energy due to the flow [19]. Specifically, for a dumbbell model without conformation-dependent drag the probability

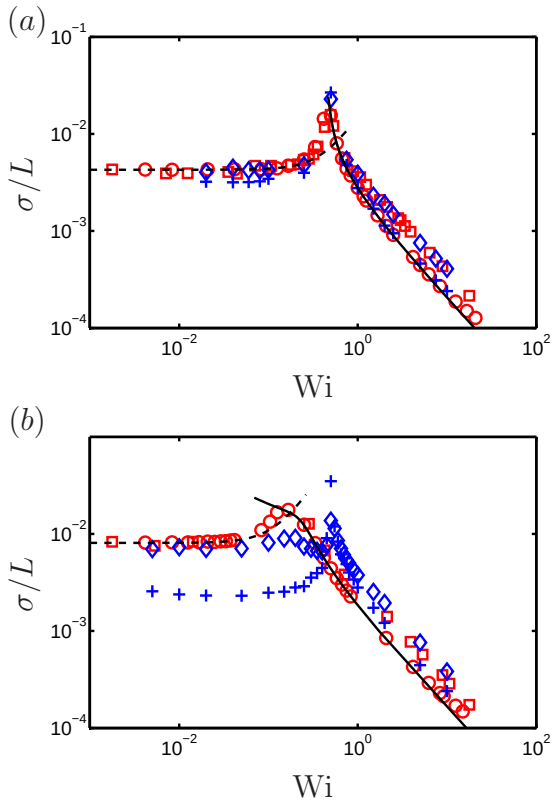

FIG. 1. (Color online) Comparison of the peaks in fluctuations between different models of (a) ds-DNA and (b)ss-DNA with no HI. σ from BD simulations of a dumbbell (◯), and 20 spring (□) chain using F_{ISEV} springs are shown in comparison against F_{FENE} spring dumbbell model (+) and 20 spring (♢) chain. σ is calculated by Eq. (14) at low Wi (dashed line) and Eq. (15) at high Wi (solid line) for the F_{ISEV} dumbbell.

density of having a spring vector $\boldsymbol{Q}$ is

$$P(\boldsymbol{Q}) = \frac{\exp(-U_{spr}/(k_BT))\exp(-\zeta\dot{\epsilon}Q^2(1-3\cos^2\theta)/(8k_BT))}{\int \exp(-U_{spr}/(k_BT))\exp(-\zeta\dot{\epsilon}Q^2(1-3\cos^2\theta)/(8k_BT))d\boldsymbol{Q}} \tag{11}$$

where θ is the angle between the $\boldsymbol{Q}$ vector and the z-axis (the extension axis of the flow) and U_{spr} is the energy in the spring (integral of the spring force) which only depends on the magnitude of the spring length Q. Applying the definition in equation 10 to a dumbbell model we see that $\sigma^2 = \langle Q^2\rangle_{fl} - \langle Q\rangle_{fl}^2$ where we use the subscript as a reminder that the average is done in flow, using the probability density in equation 11. For small strain rates, we can expand the exponential in a Taylor series in small $\dot{\epsilon}$, and write the probability density and averages in terms of the equilibrium values

$$P_{eq}(\boldsymbol{Q}) = \frac{\exp(-U_{spr}/(k_BT))}{\int \exp(-U_{spr}/(k_BT))d\boldsymbol{Q}} \tag{12}$$

$$P(\boldsymbol{Q}) \simeq P_{eq}(\boldsymbol{Q}) \frac{1 - \zeta\dot{\epsilon}Q^2(1-3\cos^2\theta)/(8k_BT) + \zeta^2\dot{\epsilon}^2Q^4(1-3\cos^2\theta)^2/(128k_B^2T^2) - \cdots}{1 + \zeta^2\dot{\epsilon}^2\langle Q^4\rangle_{eq}\langle(1-3\cos^2\theta)^2\rangle_{eq}/(128k_B^2T^2) - \cdots} \tag{13}$$

where we do not show the higher order terms for simplicity and we use a subscript to denote an average using the equilibrium distribution. Note that the term in the denominator linear in strain rate vanished because the equilibrium average of $(1-3\cos^2\theta)$ is zero. Using this series to compute the moments $\langle Q^2\rangle_{fl}$ and $\langle Q\rangle_{fl}$ in flow, we can develop a series approximation for the fluctuations near equilibrium using only equilibrium averages. This low strain rate response can be written as

$$\begin{aligned}
\sigma^2 &= \langle Q^2\rangle_{eq} - \langle Q\rangle_{eq}^2 \\
&+ \frac{1}{160}\left(-\langle Q^2\rangle_{eq}\langle Q^4\rangle_{eq} + \langle Q^6\rangle_{eq} + 2\langle Q^4\rangle_{eq}\langle Q\rangle_{eq}^2 - 2\langle Q\rangle_{eq}\langle Q^5\rangle_{eq}\right)\left(\frac{\zeta\dot{\epsilon}}{k_BT}\right)^2 \\
&+ \frac{1}{6720}\left(-\langle Q^2\rangle_{eq}\langle Q^6\rangle_{eq} + \langle Q^8\rangle_{eq} + 2\langle Q^6\rangle_{eq}\langle Q\rangle_{eq}^2 - 2\langle Q\rangle_{eq}\langle Q^7\rangle_{eq}\right)\left(\frac{\zeta\dot{\epsilon}}{k_BT}\right)^3 \\
&+ \mathcal{O}(\dot{\epsilon}^4)
\end{aligned} \tag{14}$$

For each of the dumbbell models using F_{ISEV} in Fig. 1 we evaluate the equilibrium averages numerically and express this series in terms of the Wi using the theta condition relaxation time. This low Wi series expansion of σ matches the simulations of ss-DNA as shown in Fig. 1 (b); this is true almost all the way up to the peak in the fluctuations. For ds-DNA the higher order terms in the expansion become important near the peak in σ.

At very high Wi, a dumbbell model will be aligned along the extensional axis of the flow and will only have small fluctuations around the point of minimum "energy" (including both the energy in the spring and the extra energy due to the flow). If we ignore the transverse fluctuations, we can compute the response of a 1D model, which simplifies the analysis. Very near the minimum total energy, the energy will be quadratic and the fluctuations are directly related to the stiffness of that quadratic. In particular, the fluctuations are

$$\sigma^2 \sim k_BT / \left(\frac{d^2U_{tot}}{dQ^2}\right)_{Q=Q_f}, \tag{15}$$

$$U_{tot} = U_{drag} + U_{spr}, \tag{16}$$

where Q is the magnitude of extension of the dumbbell, $U_{drag} = -k_BT\zeta_0\dot{\epsilon}Q^2/4$, U_{spr} is obtained from the integral of the spring force and Q_f is where U_{tot} is a minimum, at which $dU_{tot}/dQ = 0$. The fluctuations from this theory, valid at high Wi, are shown in Fig. 1.

The combination of low and high Wi expansions not only give a quantitative understand-

ing of the fluctuations in those limits, but also give a qualitatively understanding of the peak in fluctuations by joining together the two expansions. We can obtain an even better physical understanding of the peaks by examining two cases: a dumbbell model with spring force $AQ^{3/2}$ over all extensions and a hypothetical molecule that is long enough to have four distinct regions in its force-extension behavior. Let us first review the physical picture from the literature for the peak in fluctuations in θ conditions, in which a Hookean spring is appropriate near equilibrium and a nonlinear spring (such as FENE) is appropriate away from equilibrium.

As mentioned earlier, a dumbbell model without conformation dependent drag in elongational flow samples a Boltzmann distribution with an effective energy due to the flow which is quadratic in Q. For a Hookean model, the spring energy is also quadratic in Q. At low strain rates, the flow weakens the effective energy well in which the dumbbell fluctuates, thereby increasing the fluctuations. This continues until $\mathrm{Wi} = 1/2$, beyond which the nonlinearities of the spring force become important, decreasing the fluctuations. This picture can be contrasted with the response of a spring whose force is $AQ^{3/2}$ for all extensions, which is shown in Fig. 2. Because of the different scalings with Q of the flow energy and spring energy, the energy landscape first dips at small Q before rising at large Q for all strain rates. For small strain rates, the dip in total energy is smaller than k_BT. For these strain rates, the fluctuations grow with increasing strain rate. At larger strain rates, the energy well moves to larger extensions and the fluctuations about this minimum become smaller. At intermediate strain rates, there is a peak in the fluctuations. This is particularly interesting because the peak is not associated with a linear region of the force relation or a steep change in average extension.

Since long molecules of ss-DNA in a good solvent have a significant "Pincus region" in which the spring force scales as $f \sim Q^{3/2}$, we expect a peak in the fluctuations when the molecule first begins to stretch away from equilibrium. This is what was seen in Fig. 1 (b). There was not a peak near $\mathrm{Wi} \sim 1/2$ when the chain nears full extension. For a spring with finite length, the finite extensibility leads to a faster decay of the fluctuations at large strain rate than the $AQ^{3/2}$ spring.

It is also illustrative to consider a hypothetical molecule that has both a significant region with $f \sim Q^{3/2}$ and a significant linear region before reaching the finite extensibility region. For a molecule to have both these regions to be distinct, it should have a large N_K with

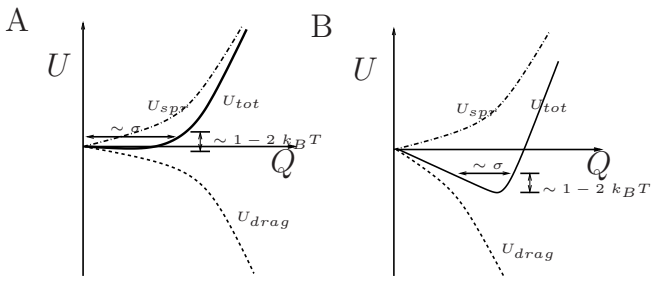

FIG. 2. Illustration of the energy landscape and fluctuations of $AQ^{3/2}$ spring at (A) low and (B) high strain rates in elongational flow. The spring is mostly restricted to regions within $1 - 2k_BT$ of the energy minimum, leading to fluctuations given by the double arrows.

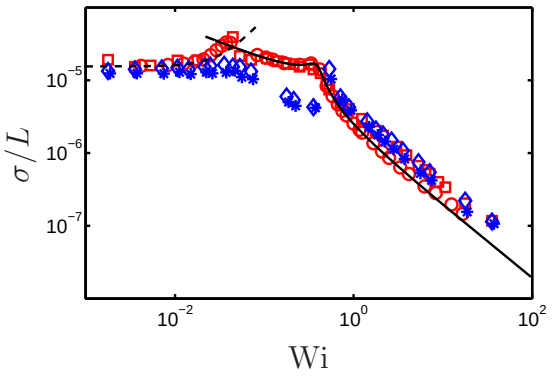

FIG. 3. (Color online) Comparison of the peaks in fluctuations between different models of a hypothetical molecule with no HI. σ from BD simulations of a dumbbell (◯), and 20 bead-spring (□) chain using F_{ISEV} springs is shown in comparison against FENE springs with EV of 10 (∗) and 20 springs (♢) chain. σ is calculated by Eq. (14) at low Wi (dashed line) and Eq. (15) at high Wi (solid line) for the F_{ISEV} dumbbell.

small v/l^3. Using the same parameters as our previous work [15], we take $v/l^3 = 0.03$ and $N_K = 10^{10}$ for the hypothetical molecule. Although there is only a single linear region in the spring force relation for this molecule, it has two peaks in σ as shown in Fig. 3. The first peak is due to the non-linear spring force and the second peak is due to the linear region in the spring force. The model with FENE springs attempting to represent this molecule shows only a single peak at Wi=0.5 due to a large linear region in the FE response. The molecules in Fig. 1 can be thought of as limiting cases of the two peak response, in which only one of the peaks is present.

A simple method to examine the influence of HI on the fluctuations is by means of a

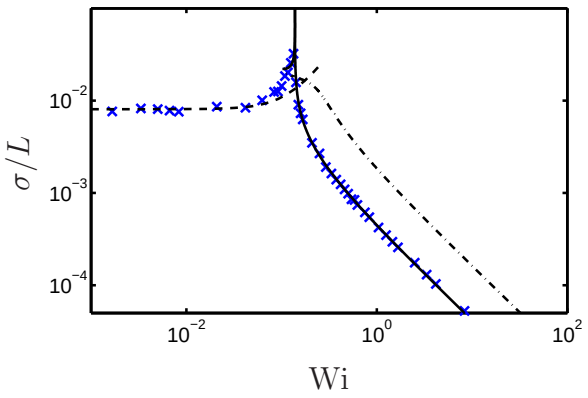

FIG. 4. (Color online) Fluctuations of F_{ISEV} dumbbell with conformation dependent drag having $N_K = 10^4$ steps and $v/l^3 = 1$. σ from BD simulations of a molecule with $\beta Q_0 = 2.89$ (x) is shown. The high Wi response matches well with Eq.15 using Eq.19 (solid line) for $\beta Q_0 = 2.89$. For comparison, the low Wi (dashed) and high Wi (dot-dashed) response without conformation dependent drag are shown, and are the same as Fig.1 (b).

dumbbell model with conformation dependent drag coefficient $\zeta(Q)$. Previous work has shown that a dumbbell model with a F_{ISEV} spring is able to capture the force extension behavior and flow response of a bead spring chain [15, 16]. We have shown here that it also captures the fluctuations in flow, so it can be used with a function $\zeta(Q)$ to examine the impact of HI on the fluctuations. The simple functional form $\zeta(Q) = \zeta_0(1 + \beta Q)$ has been used previously to capture the important features of the conformation dependent drag [1, 16], where β is a constant determined by

$$1 + \beta Q_0 \approx \frac{\sqrt{\frac{2}{3}\frac{R_\theta^2}{\langle Q^2\rangle_{Eq}} N_K}}{(log(l/d) + log(N_K))} \ , \tag{17}$$

where d is the polymer backbone hydrodynamic diameter and $\langle Q^2\rangle_{Eq}$ is evaluated using an approximate relation for good solvents [21, 22]

$$\left(\frac{\langle Q^2\rangle_{Eq}}{R_\theta^2}\right)^{5/2} - \left(\frac{\langle Q^2\rangle_{Eq}}{R_\theta^2}\right)^{3/2} = \sqrt{\frac{6N_K}{\pi^3}}\frac{v}{l^3} \ . \tag{18}$$

A key parameter that determines the importance of conformation dependent drag is βQ_0. If $\beta Q_0 \ll 3$, then the drag coefficient is almost the same for all configurations and the peak in the fluctuations will not be affected by conformation dependent drag. If $\beta Q_0 > 3$, there can be hysteresis in the CST, which has been examined in detail previously [16]. Measuring the fluctuations within the hysteresis loop is not the goal of this work. Even before the onset

of hysteresis, conformation dependent drag can impact the fluctuations. At large Wi, σ with conformation dependent drag can be understood from the 1D energy landscape analysis. For a 1D model with conformation dependent drag, Eq. 15 is applicable at high Wi by taking

$$U_{drag} = -k_B T \zeta_0 \dot{\epsilon} (Q^2/4 + \beta Q^3/6) \tag{19}$$

in Eq.16. A molecule such as ss-DNA with aspect ratio $l/d = 1$, $v/l^3 = 1$ and $N_K = 10^4$ has an estimated $\beta Q_0 = 2.89$. The fluctuations of such a molecule is shown in Fig. 4. For comparison, we show the approximate low and high Wi behavior when $\beta = 0$. At low Wi, we see that the nonzero β causes the fluctuations to increase with Wi more rapidly than when $\beta = 0$. At high Wi, the conformation dependent drag decreases the fluctuations and leads to a steeper peak in the fluctuations. Since $\zeta(Q)$ has a significant impact on σ, more accurate models for $\zeta(Q)$ developed in comparison with experiments will be important to predict the exact response.

IV. CONCLUSIONS

In conclusion, using BD simulations in elongational flow we have shown that a peak in the fluctuations σ is not necessarily associated with a linear region in the spring force relation or a sharp change in extension of the molecule. Even a non-linear force relation associated with the "Pincus region" of the force extension behavior could give rise to a peak in the fluctuations. We used the recently developed F_{ISEV} model which incorporates intraspring excluded volume forces into the spring force. Because this spring force accurately captures the elasticity of the chain, a very coarse model can be used, which speeds the computations and allows for simpler analysis. We find that a peak in σ does not always indicate a sharp transition from a coiled state to a stretched state. Conformation dependent drag leads to enhancement in σ and the high strain rate response of σ can be understood by taking the second derivative of the potential energy U_{tot} with respect to extension of a 1D dumbbell model. Our results suggest that single molecule experiments involving flexible molecules in good solvents, such as ss-DNA, in elongational flow will show different fluctuations than

previous work on ds-DNA.

[1] J. Tang, D. . Trahan, and P. S. Doyle, Macromolecules **43**, 3081 (2010).

[2] K. D. Dorfman, S. B. King, D. W. Olson, J. D. P. Thomas, and D. R. Tree, Chemical Reviews **113**, 2584 (2013).

[3] D. J. Mai, C. Brockman, and C. M. Schroeder, Soft Matter **8**, 10560 (2012).

[4] P. S. Virk, AIChE J. **21**, 625 (1975).

[5] C. M. White and M. G. Mungal, Annu. Rev. Fluid Mech. **40**, 235 (2008).

[6] P. G. De Gennes, J. Chem. Phys. **60**, 5030 (1974).

[7] E. J. Hinch, Phys. Fluids **20**, S22 (1977).

[8] C. M. Schroeder, H. P. Babcock, E. S. G. Shaqfeh, and S. Chu, Science **301**, 1515 (2003).

[9] T. Sridhar, D. A. Nguyen, R. Prabhakar, and J. R. Prakash, Phys. Rev. Lett. **98**, 167801 (2007).

[10] S. Gerashchenko and V. Steinberg, Phys. Rev. E **78**, 040801 (2008).

[11] P. Pincus, Macromolecules **9**, 386 (1976).

[12] O. A. Saleh, D. B. McIntosh, P. Pincus, and N. Ribeck, Phys. Rev. Lett. **102**, 68301 (2009).

[13] D. B. McIntosh, N. Ribeck, and O. A. Saleh, Phys. Rev. E **80**, 41803 (2009).

[14] A. Dittmore, D. B. McIntosh, S. Halliday, and O. A. Saleh, Phys. Rev. Lett. **107**, 148301 (2011).

[15] R. Radhakrishnan and P. T. Underhill, Soft Matter **8**, 6991 (2012).

[16] R. Radhakrishnan and P. T. Underhill, Macromolecules **46**, 548 (2013).

[17] H. C. Ottinger, *Stochastic Processes in Polymeric Fluids* (Springer-Verlag, Berlin, 1996).

[18] H. Warner Jr, Ind. Eng. Chem. Fundam. **11**, 379 (1972).

[19] R. B. Bird, R. C. Armstrong, O. Hassager, and C. F. Curtiss, *Dynamics of Polymeric Liquids*, vol. 2 (Wiley, New York, 1987).

[20] P. T. Underhill and P. S. Doyle, J. Non-Newtonian Fluid Mech. **145**, 109 (2007).

[21] H. Yamakawa, *Modern theory of polymer solutions* (Harper & Row, New York, 1971).

[22] M. Doi and S. F. Edwards, *The Theory of Polymer Dynamics* (Oxford University Press, New York, 1988).